Magnetic-field and temperature dependence of the thermally activated dissipation in thin films of $Bi_2Sr_2CaCu_2O_{8+\delta}$

J. T. Kucera* and T. P. Orlando†
Massachusetts Institute of Technology, Cambridge, Massachusetts 02139

G. Virshup and J. N. Eckstein
Varian Research Center, Palo Alto, California 94304
(Received 29 April 1992)

The resistive transitions of a wide variety of $Bi_2Sr_2CaCu_2O_{8+\delta}$ thin films have been measured in $\mu_0\mathbf{H}\|\hat{\mathbf{c}}$ from 0.01 to 15 T. For all samples, the transitions can be well approximated by the thermally activated form: $R(T,H)\approx R_n\exp\{-A(1-T/T_c)/k_BT\sqrt{H}\}$ in the range $10^{-6}R_n<R<10^{-2}R_n$. The energy scale A is 1740 K for smooth, *in situ* films made by molecular-beam epitaxy, and is 890 K for rough, polycrystalline films made by ambient temperature sputtering with an *ex situ* anneal. The field and temperature dependence of the activation energy, as well as its overall magnitude, is consistent with a model in which $U(T,H)$ arises from plastic deformations of a viscous flux liquid above the vortex-glass transition temperature. The flux lattice shear mechanism proposed by this model is shown to be energetically preferable to direct lattice shear in highly anisotropic materials, thus explaining why the activation energy in $Bi_2Sr_2CaCu_2O_{8+\delta}$ has a different field dependence than that for $YBa_2Cu_3O_7$.

I. INTRODUCTION

The resistive transitions of all high transition temperature superconductors broaden in applied magnetic fields.[1-3] This broadening exists in the limit of zero current, and is more pronounced in more highly anisotropic materials. The broadening is widely believed to result from the thermally assisted motion of magnetic flux, except perhaps near T_c, where fluctuations of the order parameter may be important. However, there is not a complete consensus on how the relatively high temperatures and strong anisotropy lead to the observed resistive transitions. This is because neither the underlying pinning mechanisms nor the high-temperature dynamics of vortices in these extremely anisotropic systems are well understood.

Experiments have shown that the broadening is thermally activated between approximately $10^{-6}R_n$ and $10^{-2}R_n$.[1-3] However, the origin of the activation energy is unknown. Despite the tremendous amount of experimental work in this area there has been little effort to systematically study the broadening of the resistive transitions on a wide variety of samples as a function of their microstructure and surface morphology. We present such a study using thin films of $Bi_2Sr_2CaCu_2O_{8+\delta}$. This material was chosen because its high anisotropy and reliable *in situ* fabrication make it an ideal model system.

Section II summarizes the properties of the *in situ* and *ex situ* films made both by sputtering and by layer-by-layer molecular-beam epitaxy (MBE). Section III describes the measurement procedure and the assumptions made in interpreting the data. The results are described in Sec. IV. The main result of this paper is that the resistive transitions of all samples can be well approximated by the thermally activated form

$$R(T,H)=R_0\exp\{-A(1-T/T_0)/k_BT\sqrt{H}\}\ , \quad (1)$$

where R_0 and T_0 are nearly equal to the normal-state resistivities R_n and transition temperatures T_c, respectively. This result will be shown to be valid in the range $10^{-6}R_n<R<10^{-2}R_n$ for $0.01\ \text{T}\le\mu_0H\le 1$ T, and for $10^{-6}R_n<R<10^{-4}R_n$ for $1\ \text{T}<\mu_0H\le 15$ T. In Sec. V we compare the experimental results to a model based on the thermally activated motion of edge dislocations in the flux lattice, and find reasonable agreement without any adjustable parameters. We argue that the type of shear in the vortex lattice is different for $Bi_2Sr_2CaCu_2O_{8+\delta}$ than for $YBa_2Cu_3O_7$, and that the vortices become three dimensional in the lowest magnetic fields and temperatures considered. Three-dimensional vortices are required for the existence of a finite-temperature vortex-glass transition as predicted by Fisher, Fisher, and Huse.[4]

II. FILM PROPERTIES

Table I summarizes the properties of the samples measured. Films were made by ambient temperature sputtering followed by an *ex situ* anneal (SPU-A and SPU-B), elevated temperature sputtering (SPU-1 and SPU-2), and layer-by-layer MBE (MBE-1 and MBE-2). All films were on (100) $SrTiO_3$ substrates except SPU-A, which was on (100) MgO. The films were from 100 to 160 nm thick, and were highly textured with the $\hat{\mathbf{c}}$ axis perpendicular to the substrate. Samples had a wide variety of surface morphologies ranging from rough and polycrystalline to atomically smooth, epitaxial, and untwinned. The resistivity of most samples at 100 K was approximately 300 $\mu\Omega$ cm, which is roughly five times that of the highest-quality single crystals.[2,5] Transport critical current den-

TABLE I. Properties of all samples measured. Films were made by ambient temperature sputtering followed by an *ex situ* anneal (SPU-A and SPU-B), elevated temperature sputtering (SPU-1 and SPU-2), and layer-by-layer MBE (MBE-1 and MBE-2). All films were on $SrTiO_3$ substrates except SPU-A, which was on MgO. Samples MBE-1 and MBE-2 represent two separate devices patterned on the same untwinned film with the current applied along the $\hat{\mathbf{a}}$ and $\hat{\mathbf{b}}$ axes, respectively. The parameters T_0 and ρ_0 are the best fits to the activated resistivity $\rho(T,H)=\rho_0\exp\{-A(1-T/T_0)/k_BT\sqrt{H}\}$.

Sample no.	Deposition technique	T_{dep} (°C)	Annealed	Surface morphology	Thickness (nm)	ρ_N (100 K) ($\mu\Omega$ cm)	T_c (K)	J_c (4.2 K) (A/cm^2)	T_0 (K)	$\frac{\rho_0}{\rho_N\ (100\,\mathrm{K})}$
SPU-A	Sputter	40	yes	rough	160	290	84	7×10^4	89.3	1.91
SPU-B	Sputter	40	yes	rough	160	740	80	5×10^4	84.0	1.23
SPU-1	Sputter	710	no	smooth	110	300	51	1×10^6	54.1	1.67
SPU-2	Sputter	680	yes	smooth	130	300	73	4×10^6	79.4	2.69
MBE-1	MBE	650	no	smooth	100	270	79	1×10^6	89.3	12.4
MBE-2	MBE	650	no	smooth	100	1900	79	1×10^6	88.5	31.2

sities (J_c) ranged from 5×10^4 A/cm^2 for *ex situ* films to greater than 10^6 A/cm^2 for *in situ* films.[6] Samples MBE-1 and MBE-2 were actually two separate devices patterned on the same untwinned film, with the current applied along the $\hat{\mathbf{a}}$ and $\hat{\mathbf{b}}$ directions, respectively.

Samples SPU-A and SPU-B were prepared by ambient-temperature sputter deposition followed by an *ex situ* anneal. This process is described in detail by Face *et al.*[7,8] These films were typical of polycrystalline, *ex situ* films in that they were extremely rough, with numerous secondary phase surface precipitates and a micaceous surface morphology.[9] The existence of weak-link grain boundaries in these films has been suggested by our ability to pattern them into dc superconducting quantum interference devices,[10] by the fact that their transport J_c's were 20 times smaller than typical intragranular J_c's,[11] and by the suppression of J_c (4.2 K) in magnetic fields of about 100 Oe applied parallel to their $\hat{\mathbf{c}}$ axes.[12] While SPU-A was representative of most *ex situ* films, SPU-B appeared to consist of a poorly connected array of weak links. Films prepared in the same deposition as SPU-B did not support any current when patterned into lines narrower than 100 μm. In addition, the resistivity of SPU-B was nearly twice that of SPU-A, suggesting that the effective cross-sectional area for current flow was a factor of 2 smaller than that of SPU-A. The current-voltage (I-V) characteristics of SPU-B exhibited a sharp voltage onset similar to that seen in single Josephson junctions. In contrast, SPU-A had a rounded voltage onset similar to that seen in all the other films.

Samples SPU-1 and SPU-2 were sputter deposited onto elevated temperature substrates in the presence of pure ozone. This process is described in detail by Kucera *et al.*[13] As-deposited films were superconducting with $R=0$ transition temperatures (T_c) of 40–50 K, and zero field J_c's of greater than 10^6 A/cm^2 at 4.2 K. Some of these films were annealed to increase their transition temperatures to near the bulk value of 80 K. Sample SPU-1, with an as-deposited T_c of 51 K, was included in the study as a control in order to understand the effects of intentional broadening due to sample inhomogeneity. Sample SPU-2 was annealed and had a transition temperature of 73 K. The surfaces of SPU-1 and SPU-2 were much smoother than those of polycrystalline *ex situ* films such as SPU-A and SPU-B.[14] As-deposited films had typical surface roughness of less than 5 nm as confirmed by high-resolution scanning tunneling microscopy. Annealed films were slightly rougher, but were still very smooth compared to SPU-A and SPU-B. The relatively large transport critical current densities in these films were comparable to the intragranular J_c's observed in $Bi_2Sr_2CaCu_2O_{8+\delta}$ microbridges,[11] suggesting that grain boundaries do not affect the transport properties of these films.

Samples MBE-1 and MBE-2 were actually two different devices patterned along the $\hat{\mathbf{a}}$ and $\hat{\mathbf{b}}$ directions, respectively, of the same untwinned film. This film was deposited layer-by-layer by molecular-beam epitaxy onto a vicinal $SrTiO_3$ substrate cut 2° off {100} towards a ⟨111⟩ direction. Details of the sample fabrication and characterization are described by Eckstein *et al.*[15,16] Step edges in the substrate resulted in untwinned growth and anisotropic transport properties. The room-temperature resistivity along the film's $\hat{\mathbf{a}}$ axis (parallel to the steps) was one-fifth that along the $\hat{\mathbf{b}}$ axis. In addition, the $\hat{\mathbf{a}}$ axis normal-state resistivity decreased more rapidly with decreasing temperature than the $\hat{\mathbf{b}}$-axis resistivity. This anisotropy might be due to the intrinsic anisotropy between ρ_a and ρ_b,[5] or to the presence of the step edges.[17] The step edges cause a small component of the current to flow along the high-resistivity $\hat{\mathbf{c}}$ direction in sample MBE-2. Films made by MBE had extremely smooth surfaces with widely dispersed outgrowths.[18] Like high-temperature sputtered films, MBE films showed no evidence for grain boundaries in their transport characteristics. The as-deposited transition temperature for both MBE-1 and MBE-2 was 80 K, and zero-field critical current densities were estimated to be greater than 10^6 A/cm^2 at 4.2 K.[19]

III. EXPERIMENTAL PROCEDURE

Most of the data were obtained by measuring the resistance as a function of temperature for various fixed magnetic fields. For the remainder of this discussion, the "resistance" will be defined to be the zero-bias resistance $dV/dI|_{I=0}$. This quantity should not be confused with the "flux-flow" resistance $dV/dI|_{I>I_c}$. The zero-bias resistance comes from the linear portion of the current-voltage characteristic near $I=0$. This quantity is

nonzero only at temperatures and fields above the vortex-glass transition.

The zero-bias resistance was measured ac at frequencies of either 25 or 519 Hz. This resistance was confirmed to be independent of the choice of measurement frequency. The modulation current was 50 μA peak-to-peak, corresponding to current densities of between 250 and 700 A/cm^2, depending on the sample geometry. The modulation current was small enough to remain within the linear portion of the I-V characteristic at all temperatures and fields. This was confirmed by measuring the I-V characteristics at a number of fixed temperatures and fields, and by remeasuring several of the resistive transitions with reduced current modulations.

For all experiments, the magnetic field was applied along the average $\hat{c}$ axis of the highly textured samples, and was perpendicular to the direction of the current. The films were patterned by wet chemical etching, into four-point resistance bridges 50–100-μm wide by 0.5–2.0-mm long. The sample temperature was measured with a calibrated carbon-glass thermometer, and accurate corrections were applied to account for its magnetoresistance in fields above 2 T.[20]

IV. EXPERIMENTAL RESULTS

In this section we will discuss the magnetic field and temperature dependence of the activation energy determined from the low-resistance portion of the transitions. First we will discuss the resistive transitions in fixed magnetic fields. These will be shown to be thermally activated for $R \ll R_n$. Then we will investigate the field and temperature dependence of the activation energy. The field dependence will be shown to be well approximated by $U \propto H^{-1/2}$ over three orders of magnitude in magnetic field. This result will be shown to hold regardless of the temperature dependence of U. The temperature dependence will be shown to go like $(1-T/T_c)$ for $\mu_0 H \leq 1$ T. For $\mu_0 H > 1$ T, the temperature dependence is less certain. We will argue that the $(1-T/T_c)$ dependence is reasonable even in this high-field regime, because it consistently explains the anomalously high prefactors to the activated resistivity,[2] and because it leads to the same field dependence for U. Finally, we will show that $R_0 \approx R_n$ and $T_0 \approx T_c$ independent of the magnetic field.

Figure 1 is an Arrhenius plot of the resistance as a function of temperature for sample MBE-1 in various fixed magnetic fields. This plot displays over six orders of magnitude in resistance, and emphasizes the lowest-temperature portions of the transition where $R \ll R_n$. The qualitative shapes of the resistive transitions of all samples studied were similar to those depicted in Fig. 1 despite the wide variety of surface morphologies and deposition techniques used to produce the films. This suggests that the mechanisms responsible for the broadening are universal to these $Bi_2Sr_2CaCu_2O_{8+\delta}$ films. The only sample with a slightly different transition was SPU-1. This sample had a reduced transition temperature, but for $R \leq 10^{-2} R_n$ its resistive transitions were similar to those of the other samples when the temperature was scaled by its reduced T_c.

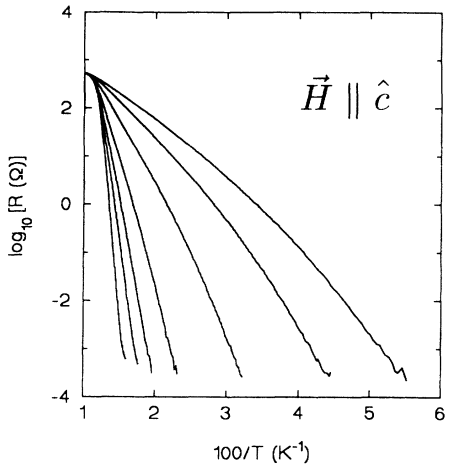

FIG. 1. Arrhenius plot of the resistive transitions of sample MBE-1 in fixed magnetic fields $\mu_0 \mathbf{H} \| \hat{\mathbf{c}} = 0.1$, 0.5, 1.0, 2.0, 5.0, 10.0, and 15.0 T (left to right). Resistive transitions of all other samples were qualitatively similar to those depicted here.

For $\mu_0 H \leq 1$ T, Arrhenius plots of the resistive transitions of all films were linear from $10^{-6} R_n - 10^{-2} R_n$. This confirmed that the resistance was thermally activated with

$$R = R_0 \exp(-U_0/k_B T) \ . \tag{2}$$

The activation energy U_0 is determined from the slope of the line tangent to the transition at the lowest-resistance portions of the curve. The prefactor R_0 is determined from the intercept of this line with $1/T = 0$.

For $\mu_0 H > 1$ T, the regime over which the Arrhenius plots remained linear shifted to lower and lower resistances with increasing magnetic field. However, even at the highest fields of 15 T, the transitions remained linear over more than two orders of magnitude in resistance. The rounding of the transitions at higher resistances may result from a nonlinear temperature dependence to the activation energy. This possibility will be considered later. For now we will define U_0 to be the slope of the Arrhenius plot of the resistive transition in the lowest-resistance regime. This approach allows us to compare the resistive transitions from several different samples and magnetic fields on the same footing. In addition, the low-resistance regime should reflect the physics of the underlying pinning mechanism, because this is where the vortices are primarily impeded by thermally assisted depinning rather than by viscous drag (flux flow).

Now we will investigate the field dependence of the activation energy. Figure 2 shows U_0 as a function of magnetic field for all the films measured, and for a bulk single crystal of $Bi_2Sr_2CaCu_2O_{8+\delta}$ measured by Palstra *et al.*[2] The activation energies of all films fell into one of two classes. Smooth *in situ* films with high J_c's had activation energies approximately twice as large as rough *ex situ* films with low J_c's.[21] The fact that rougher films had lower activation energies indicates that flux pinning was not enhanced by roughness. One would not expect pin-

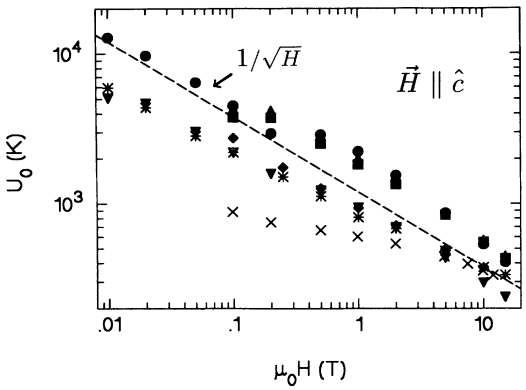

FIG. 2. Activation energy as a function of field for films MBE-1 (■), MBE-2 (▲), SPU-1 (▼), SPU-2 (●), SPU-A (*), and SPU-B (♦), compared to that of a bulk single crystal (×) measured by Palstra *et al.* (Ref. 2). The field dependence of the activation energy of the films is well approximated by $U_0(H) \propto 1/\sqrt{H}$.

ning to be enhanced by the second phase precipitates because they are much larger than the coherence length (ξ). However, the voids and terraced surface topography might be expected to enhance the pinning in rough films. Our results show that neither of these effects are important in determining the activation energies.

The activation energy was most strongly correlated with J_c for the thin-film samples. This is not surprising because the activation energy is determined by the height of the pinning barrier, while the critical current density is determined by its slope. The activation energies of the films were greater than or equal to those of the bulk single crystal. It was impossible to determine if the correlation with J_c applied to the crystal, however, because its critical current density was not reported.

For both classes of films, the activation energy followed a power law $U_0 \propto H^{-\alpha}$ over three orders of magnitude in field. For the higher activation energy class of films, $\alpha = 0.45$ and U_0 (1 T) = 1740 K. For the lower activation energy class of films, $\alpha = 0.41$ and U_0 (1 T) = 890 K. The fact that the field dependence observed for $\mu_0 H \leq 1$ T extended to $\mu_0 H > 1$ T supports the interpretation that the activation energy should be determined from the lowest-resistance portions of the transitions when $\mu_0 H > 1$ T.

We have shown $U_0(H)$ to be a power law over more than three orders of magnitude in magnetic field. Most other measurements have been performed only over one or two orders of magnitude in field. Even then, the results fit a power law only over a small portion of the range of fields measured. The activation energy of the bulk single crystal depicted in Fig. 2 is typical of other measurements. For $H < 3$ T, the power law is $\alpha = 0.16$, while for $H > 3$ T, $\alpha = 0.33$.

The strong field dependence of the activation energy suggests some form of collective pinning. An intuitive model proposed by Tinkham[22] predicts

$$U \propto \tfrac{1}{2}\mu_0 H_c^2 \xi^n a_0^m , \quad (3)$$

where $\frac{1}{2}\mu_0 H_c^2$ is the condensation energy per unit volume, and the volume has some power of the average intervortex spacing $a_0 \approx \sqrt{\Phi_0/B}$. This expression is valid for $H_{c1} \ll H \ll H_{c2}$. In Tinkham's model, the activation energy is the energy required for a correlated volume of flux to shear past neighboring vortices. The energy is related to the free-energy difference between the normally triangular flux lattice and the square flux lattice created during the displacement. The exponent for the activation energy is expected to be $\alpha = (3-m)/2$, where $m = 0$–3. The limiting form $m = 0$ also corresponds to the expression for core pinning of *independent* vortices. *Because the observed values of* α *are much closer to* $\frac{1}{2}$ *than to 1 or* $\frac{3}{2}$ *we will approximate the activation energy by* $U \propto 1/\sqrt{H}$ *for the remainder of this discussion.* This approximation is reasonable given the scatter of the experimental data points in Fig. 2.

Field dependences of roughly $1/\sqrt{H}$ have also been seen by Woo *et al.*[23] in one polycrystalline TBCCO film, and by White, Kapitulnik, and Beasley[24] in a quasi-two-dimensional multilayer sample of Mo-Ge/Ge in the limit of weak Josephson coupling. This contrasts with the $1/H$ field dependence, which is typically seen in YBCO films and crystals.[3,25] In $Bi_2Sr_2CaCu_2O_{8+\delta}$ films, field dependences of roughly $1/\sqrt{H}$ have been found in certain very limited field regimes,[26,27] but the activation energies for these results were determined over less than two orders of magnitude in resistance, and in the high-resistance portions of the transitions where the broadening may not be thermally activated. There have been several other reports of activation energies following a $1/\sqrt{H}$ field dependence in bulk $Bi_2Sr_2CaCu_2O_{8+\delta}$ (Ref. 28) and $Tl_2Ba_2Ca_2Cu_3O_{10+\delta}$ (Ref. 29) powders, and in Pb-doped $Bi_2Sr_2Ca_2Cu_3O_{10+\delta}$ films,[30] but these measurements have been performed only over roughly one order of magnitude in field and in very limited ranges of resistances.

It is surprising that the $1/\sqrt{H}$ field dependence extends to fields as small as 0.01 T. The intervortex separation would be expected to become larger than the typical *a-b* penetration depth (λ_{ab}) in fields smaller than 0.1 T, eliminating the possibility of collective pinning. However, the low-field data is taken at temperatures close to T_c, where $\lambda_{ab}(T)$ begins to diverge like $(1-T/T_c)^{-1/2}$. For $\mu_0 H = 0.01$ T, the entire transition was measured at temperatures above 76 K. Using the experimentally determined value of $\lambda_{ab}(0)$ in $Bi_2Sr_2CaCu_2O_{8+\delta}$ of ≈ 3000 Å,[31,33] $\lambda_{ab}(T) \geq 5000$ Å for $T \geq 76$ K. Thus, the intervortex spacing remains less than the penetration depth and collective pinning is possible. In fields below 0.01 T, the activation energy falls below the $1/\sqrt{H}$ line, as would be expected from a crossover to individual vortex pinning. The largest value of a_0/λ_{ab} that is consistent with collective pinning depends on the strength of the individual forces relative to the intervortex forces. The individual pinning forces are expected to be greatly reduced by thermal fluctuations for temperatures near T_c.[34] Therefore it may be possible to observe collective pinning for values of a_0/λ_{ab} slightly greater than 1.

The $1/\sqrt{H}$ field dependence was confirmed by mea-

surements of the resistance as a function of field at various fixed temperatures. Figure 3 is a plot of $\log_{10}(R)$ versus $1/\sqrt{H}$ for sample SPU-A. This data was taken by fixing the temperature and increasing the magnetic field from zero to 5 or 10 T. The transitions are linear over the lowest three orders of magnitude in resistance, confirming that $R \propto \exp(-A/\sqrt{H})$ in this regime. This shows that the activation energy is proportional to $1/\sqrt{H}$ regardless of its temperature dependence.

Now we return to discuss the temperature dependence of the activation energy. The thermally activated model has been assumed to hold only for the lowest-resistance portions of the transitions where the Arrhenius plots are linear. This implies that the activation energy is either constant or linearly dependent on temperature. It is also possible that the resistive transitions are thermally activated over a larger range of resistivities, and that the nonlinear Arrhenius plots for $\mu_0 H > 1$ T result from a nonlinear $U(T)$. In this case, the activation energy can be obtained by inverting expression (2). This gives

$$U(T,H) = -k_B T \ln\left\{\frac{R(T,H)}{R_0}\right\} . \tag{4}$$

Figure 4 shows the activation energy as a function of temperature for sample MBE-1. For this graph, R_0 has been taken to be the linear extrapolation of the normal-state resistance to below T_c. This choice is physically reasonable, and it allows $U(T)$ to go to zero at T_c. The resulting $U(T)$ is relatively insensitive to the choice of R_0 so long as R_0 is not exponentially dependent on temperature.

For fields less than or equal to 1 T, the activation energy is linear in temperature over most of the transition and extrapolates to zero at T_c. For higher fields, the activation energy is given by the nonlinear function depicted. This function has an unusual upward kink for $T \leq T_c/2$ in the highest-field transitions. The activation energy regains its linear temperature dependence in the higher activation energy portions of these curves. This corresponds to the low-resistance portions of the Arrhenius plot depicted in Fig. 1, and is the regime where $U \gg k_B T$. This is where the vortex motion is expected to be determined by thermally activated hopping. The dashed line in Fig. 4 separates the regime of linear (above the line) and nonlinear (below the line) $U(T)$.

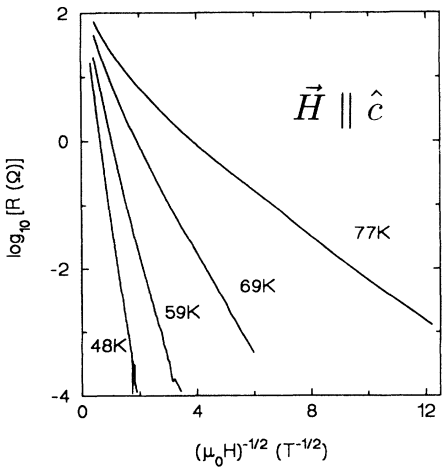

FIG. 3. Resistance as a function of field for sample SPU-A at various fixed temperatures. Higher fields are closer to the origin on this graph of $\log_{10}(R)$ vs $1/\sqrt{H}$.

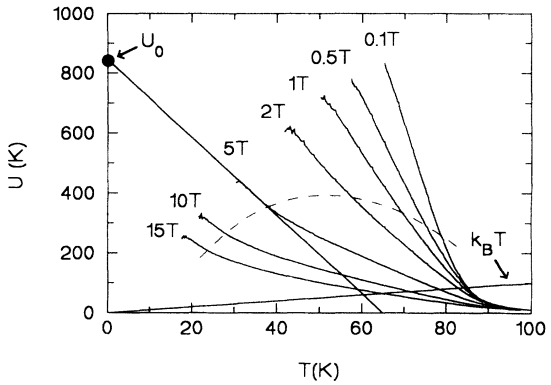

FIG. 4. Activation energy as a function of temperature for sample MBE-1 in $\mu_0 \mathbf{H} \| \hat{\mathbf{c}} = 0.1$ 0.5, 1.0, 2.0, 5.0, 10, and 15 T. Lines of constant resistance pass through the origin with increasing slope for smaller resistances. The activation energy is nearly linear in temperature in the low-resistance regime above the dashed line.

The nonlinear portions of $U(T)$ are not consistent with that predicted by Eq. (3). Using the conventional temperature dependences for H_c and ξ, the activation energy becomes

$$U(t) \propto (1-t^2)^{2-n/2}(1+t^2)^{n/2} , \tag{5}$$

where $t \equiv T/T_c$ and $n = 0$–3 is the power of ξ in Eq. (3). Only the $n = 0$ curve has the correct curvature below T_c. However, none of the curves can account for the sudden upward kink in the observed $U(t)$ below $t = \frac{1}{2}$. This kink cannot be explained by any model using the conventional superconducting length or energy scales because none of them change rapidly for $t \leq \frac{1}{2}$.

It is possible that the kink represents a transition between different regimes of behavior. One possibility is that the kink is a crossover from thermally activated flux motion to flux flow. However, this crossover occurs at too low of a resistance to be consistent with the flux-flow resistivity $\rho_f = \rho_n H/H_{c2}$, unless H_{c2} is much larger than has been previously estimated. Another possibility is that the kink is a crossover from three-dimensional (3D) to 2D behavior as the temperature is increased. This possibility will be discussed further in Sec. V. A sudden increase in the activation energy at low temperatures has also been seen by Safar *et al.*[35] in a bulk single crystal of $Bi_2Sr_2CaCu_2O_{8+\delta}$.

As was pointed out by Beasley, Labusch, and Webb,[36] the activation energy obtained from the slope of the Arrhenius plot is the $T = 0$ extrapolation of the line tangent to U at the temperature at which the slope is measured. Thus the values plotted in Fig. 2 are actually the extrapo-

lation of the low-resistance linear portions of $U(T)$ to $T=0$. This is equivalent to $U(T=0)$ if the activation energy is linear in temperature below some critical resistance. Although the data presented in Fig. 4 suggest this interpretation, it is not known whether the activation energies remain linear all the way to $T=0$ because of the finite resistance sensitivity in these experiments.

The data shown in Fig. 4 shows that $U(T) \sim (1-T/T_c)$ for $\mu_0 H \leq 1$ T. This plot is typical of all samples measured, showing that the activation energy is linear in this regime. The linear temperature dependence near T_c has been confirmed by plotting the slopes of the fixed temperature transitions shown in Fig. 3.

The most compelling evidence for a linear temperature dependence to U is provided by the prefactors R_0 obtained from the intercept of the tangent lines to Fig. 1. For all samples, R_0 is found to be from 3 to 20 orders of magnitude greater than R_n. In addition, R_0 varies with field as $\exp(c/\sqrt{H})$. Either we must postulate a separate physical mechanism to explain this peculiar magnitude and field dependence, or we can simply explain it as originating from a linear component to the activation energy. In other words, if

$$U(T)=g(H)(1-T/T_0)\ , \tag{6}$$

then

$$\ln(R)=\ln(R_0)+\frac{g(H)}{k_B T_0}-\frac{g(H)}{k_B T}\ , \tag{7}$$

and the intercept of the tangent line

$$I_t=\ln(R_0)+\frac{g(H)}{k_B T_0}\ . \tag{8}$$

The second term in (8) explains why the intercept is greater than $\ln(R_0)$ and is field dependent. However, it requires another fitting parameter T_0. This parameter cannot be obtained independent of R_0. Figure 4 suggests that $T_0=T_c$, at least for the low-field transitions, but an independent test of this idea can be performed. If both R_0 and T_0 are assumed to be independent of the field, then a plot of I_t versus the slope of the tangent line

$$S_t \equiv -g(H)/k_B \tag{9}$$

should yield a straight line whose intercept determines R_0, and whose slope determines T_0.

Figure 5 is a plot of I_t versus S_t for three representative samples. All points from a given sample lie on a straight line, supporting the assumption that R_0 and T_0 are independent of field. The slopes and intercepts of these straight lines determine the sample specific R_0's and T_0's in Eqs. (1) and (6). The values of T_0 and R_0/R_n determined for each sample are listed in Table I. For all films, T_0 is within 5 to 10 K of T_c, and R_0 is within an order of magnitude of R_n. This shows that

$$R(T,H)\approx R_n \exp\{-A(1-T/T_c)/k_B T\sqrt{H}\} \tag{10}$$

is a good approximation of the resistive transitions for all samples measured, where R_n and A are independent of field.

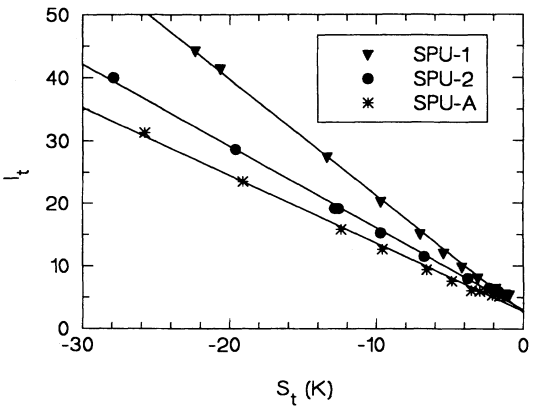

FIG. 5. Plot of the intercept (I_t) vs the slope (S_t) of the tangent lines to the Arrhenius plots for samples SPU-1, SPU-2, and SPU-A.

V. COMPARISON WITH MODELS

In this section we show that a model of plastic shear of the flux lattice explains many aspects of our data for $Bi_2Sr_2CaCu_2O_{8+\delta}$, both qualitatively and quantitatively. Moreover, by comparing other mechanisms for shear, we suggest that the highly anisotropic $Bi_2Sr_2CaCu_2O_{8+\delta}$ is dominated by plastic flux lattice shear, which gives a $1/\sqrt{H}$ dependence to the activation energy, whereas the less anisotropic $YBa_2Cu_3O_7$ is dominated by a type of shear which gives a $1/H$ dependence to the activation energy. We also argue that the vortices become three dimensional in the thermally activated regime, making it reasonable to consider the possibility of a finite temperature vortex-glass transition in this otherwise 2D material.

The experimental data show that the activation energy is well approximated by a $1/\sqrt{H}$ field dependence. Most models that predict this field dependence are variations of Tinkham's original proposal [Eq. (3)], in which the correlation volume contains one factor of the average intervortex spacing a_0 and two factors of the coherence length ξ^2. These models also predict the observed $(1-T/T_c)$ temperature dependence of U near T_c. However, these models offer no explanation of why the correlation volume should be given by $\xi^2 a_0$.

One model that does give a physical reason for the $1/\sqrt{H}$ field dependence was proposed by Geshkenbein *et al.*[37] and later extended by Vinokur *et al.*[38] This model also provides a natural explanation of why U should be lower in more highly anisotropic materials. In addition, it predicts the correct activation energies and prefactors without any independent parameters. In this model, the activated process is analogous to the thermally activated motion of edge dislocations in crystals.[39] Plastic deformations of crystal lattices do not occur via the shear of entire rows of atoms, but rather occur primarily by the motion of edge dislocations.[40] Thermal fluctuations can overcome the barriers to edge dislocation motion, but do not act coherently along the entire slip plane. Instead,

double kinks are created along the length of the dislocation. Once the kinks have nucleated, shear forces straighten them out, and the edge dislocation ends up in the next row of atoms. When the dislocation has propagated to the edge, the entire crystal has sheared by one unit cell.

In Geshkenbein's model the dislocation is in the flux lattice, and the vortex cores are analogous to the lines of dislocated atoms. Dislocations in the triangular flux lattice are moved by thermally overcoming the energy required to move a portion of the vortex into the neighboring minimum-energy position. The energy barrier for thermally assisted plastic flux lattice shear is given by the energy required to create a double kink in the vortex. Using anisotropic Ginzburg-Landau theory, the double-kink energy is[37]

$$U_{\rm pl}=2\mathcal{E}_v a_0 \approx \frac{2\Phi_0^2}{4\pi\mu_0\tilde{\lambda}^2}\ln(\tilde{\kappa})\left[\frac{\Phi_0}{B}\right]^{1/2}. \tag{11}$$

Here $\mathcal{E}_v$ is the vortex energy per unit length *along the Cu-O planes*

$$\tilde{\lambda}^2=\lambda_{ab}\lambda_c \tag{12}$$

and

$$\tilde{\kappa}=\left[\frac{\lambda_{ab}\lambda_c}{\xi_{ab}\xi_c}\right]^{1/2}. \tag{13}$$

Not only does this expression predict the $1/\sqrt{H}$ field dependence observed in the activation energy, but also it predicts the $(1-T/T_c)$ temperature dependence near T_c.

For $Bi_2Sr_2CaCu_2O_{8+\delta}$, the experimentally determined values of $\lambda_{ab}=2700$ Å,[31] $\xi_{ab}=31$ Å, [41] and $m_c/m_{ab}=6400$,[32] lead to a double-kink energy of $U_{\rm pl}(1T)=2710$ K. This is within a factor of 2 of the observed value of 1740 K in high-J_c films, and requires no independent parameters. On the other hand, $m_c/m_{ab}\approx 3000$ has also been reported for $Bi_2Sr_2CaCu_2O_{8+\delta}$[42] yielding $U_{\rm pl}(1T)=3790$ K. Our high-J_c films are expected to be more representative of the intrinsic material than the low-J_c films because the low-J_c films probably contain grain boundaries. However, the variation in the activation energy between the high-J_c and low-J_c films is not readily understood in terms of the double-kink model.

Since $\lambda_c=\lambda_{ab}\sqrt{m_c/m_{ab}}$, Eq. (11) predicts that $U_{\rm pl}\sim\sqrt{m_{ab}/m_c}$. This qualitatively explains why the activation energies observed in more highly anisotropic compounds like $Bi_2Sr_2CaCu_2O_{8+\delta}$ and $Tl_2Ba_2CaCu_2O_{8+\delta}$ are much smaller than those observed in $YBa_2Cu_3O_7$. Typical values of U_0 (1 T) in $Tl_2Ba_2CaCu_2O_{8+\delta}$ films and $Tl_2Ba_2Ca_2Cu_3O_{10+\delta}$ bulk powders range from 1500–3700 K.[23,29,43] Using the experimentally determined values of $\lambda_{ab}=2520$ Å,[31] and $m_c/m_{ab}=10^5$,[44] and assuming $\xi_{ab}=25$ Å, the activation energy is $U_{\rm pl}$ (1 T) $=920$ K. Although this value does not agree with the experimental results, the enormous effective-mass anisotropy predicts an unphysically small value of $\xi_c<0.1$ Å, which questions the validity of the experimental parameters. For $YBa_2Cu_3O_7$, $\lambda_{ab}=1400$ Å,[45–47] $\xi_{ab}=16$ Å,[48] and $m_c/m_{ab}=26$,[49] yielding $U_{\rm pl}$ (1 T) $=1.1\times10^5$ K. This is much higher than the observed values of 20 000–40 000 K,[3,25,50] suggesting that there is a lower-energy excitation. A different excitation mechanism is also suggested by the fact that the field dependence of the activation energy in $YBa_2Cu_3O_7$ follows a $1/H$ dependence,[3,25,50] rather than $1/\sqrt{H}$ as seen in $Bi_2Sr_2CaCu_2O_{8+\delta}$ and $Tl_2Ba_2CaCu_2O_{8+\delta}$.[23,29] The activation energy in $YBa_2Cu_3O_7$ is thought to arise from Tinkham's[22] model of flux lattice shearing [Eq. (3)], where the vortex dislocation moves without kinking. In Tinkham's model, the correlation volume is $N_1N_2a_0^2\xi_{ab}$, where N_1 is the number of vortices that move together along a $\hat{\mathbf{c}}$-axis length of $N_2\xi_{ab}$. The a_0^2 term gives rise to the $1/H$ field dependence. Comparing Tinkham's expression for the energy of lattice shearing to that of Geshkenbein's double-kink mechanism gives

$$\frac{U_{\rm shear}}{U_{\rm pl}}=\delta\left[\frac{1}{\beta_A}\right]\frac{\sqrt{m_c/m_{ab}}}{4\pi\ln(\tilde{\kappa})}\frac{N_1N_2}{2}\frac{a_0}{\xi_{ab}}, \tag{14}$$

where $\delta(1/\beta_A)\approx 0.02$ is the difference in the Abrikosov parameters for the square and triangular lattices. When $U_{\rm shear}/U_{\rm pl}>1$, double-kink activation is preferred. This ratio diminishes with increasing field, until direct lattice shearing is favored. In $YBa_2Cu_3O_7$, the Tinkham mechanism is favored for fields $B_x>0.4(N_1N_2)^2$ (mT). Brunner *et al.*[51] determined that the vortex correlation length along the $\hat{\mathbf{c}}$ axis was greater than 450 Å by measuring the increase in activation energy with layer thickness in YBCO/PBCO multilayers. This gives $B_x\approx 0.6$ T. However, Hettinger *et al.*[50] obtained $N_1N_2\approx 2$, giving $B_x\approx 1.6$ mT. In either case, direct lattice shearing has a lower energy than the double-kink activation in $YBa_2Cu_3O_7$ over most of the measured field range. The higher mass anisotropy for $Bi_2Sr_2CaCu_2O_{8+\delta}$ and $Tl_2Ba_2CaCu_2O_{8+\delta}$ makes the double-kink energy smaller than the direct shearing energy for $B<15$ T. Using the correlation length of $N_2=38$ determined from $YBa_2Cu_3O_7$ multilayers, $B_x\approx 18$ T for $Bi_2Sr_2CaCu_2O_{8+\delta}$, and $B_x\approx 280$ T for $Tl_2Ba_2CaCu_2O_{8+\delta}$. Thus, it appears that the Geshkenbein model with its $1/\sqrt{H}$ field dependence is applicable to $Bi_2Sr_2CaCu_2O_{8+\delta}$ and $Tl_2Ba_2CaCu_2O_{8+\delta}$, but the Tinkham model with a $1/H$ field dependence is applicable to $YBa_2Cu_3O_7$.

Vinokur *et al.*[38] have extended the Geshkenbein model by incorporating the idea of a vortex glass at low temperatures, and the transition to flux flow at high temperatures. Thermal activation still controls the motion of vortices between the vortex-glass state and the flux-flow state, but the vortices are thought of as a viscous flux liquid rather than as a lattice in the transition region.

We know our experimental data was taken within the viscous liquid regime for three reasons. First, we were above the individual vortex depinning temperature T_p defined by $k_BT_p=(\Phi_0^3Bm_{ab}/m_c)^{1/2}/\pi\mu_0\kappa^2$.[34,38] This temperature was approximately 3 K at 1 T, using the above values for ξ_{ab}, λ_{ab}, and m_c/m_{ab}. Second, we were above the vortex-glass transition because the zero-bias resistance was finite, and because the activation energy

was independent of the current. Finally, we were below the flux-flow regime, which begins at $\rho_{\rm flow}=\rho_n H/H_{c2}\approx 0.03\rho_n$ for $H\approx 1$ T.

Vinokur *et al.*[38] calculated the prefactor for the thermally activated resistivity $\rho=\rho_0\exp(-U/k_BT)$ in the viscous vortex liquid as

$$\rho_0=\rho_{\rm flow}\frac{j_0}{j_c(T_{\rm cr})}\frac{\xi_{ab}}{a_0}\left[\frac{k_BT_{\rm cr}}{2U_{\rm pl}(T_{\rm cr})}\right]^{1/2}, \tag{15}$$

where j_0 is the depairing critical current density, and $T_{\rm cr}$ is the crossover temperature determined from $\rho(T_{\rm cr})=\rho_{\rm flow}$. By assuming $\rho_{\rm flow}=\rho_n H/H_{c2}$, theoretical values of ρ_0 are found that range from $0.1\rho_n$ to ρ_n, depending on the magnetic field. These values compare favorably to the range of ρ_n to $30\rho_n$, which were experimentally observed. Because the field variation is relatively small on a logarithmic scale, the experimental data does not completely rule out such a field dependence given by $\rho_{\rm flow}$. On the other hand, the expression for traditional flux-flow resistance $\rho_{\rm flow}=\rho_n H/H_{c2}$ is not experimentally valid for $T\approx T_c$. In this regime the flux-flow resistivity has been experimentally observed to increase sharply as the phase boundary is approached.[52–54] Also, the field dependence of $\rho_{\rm flow}$ is not well supported by the experimental data. The regime of activated behavior shifts to *lower* temperatures as the magnetic field is increased, whereas the crossover temperature $\rho(T_{\rm cr})=\rho_{\rm flow}$ shifts to *higher* temperatures with increasing field.

Both Geshkenbein's original model and Vinokur's extension assume that the vortices can be described by anisotropic Ginzburg-Landau theory. This theory is inherently three dimensional because vortices extend all the way through the sample along the direction of the magnetic field. It has been proposed that in the limit of large fields and high temperatures, the conventional notion of a flux line breaks down for these highly anisotropic superconductors.[55] Instead, the vortices are described as two-dimensional "pancakes" which exist only on the copper-oxide planes.[56] This would alter Eq. (11) for the double-kink energy. In the limit of zero Josephson coupling between pancake vortices on adjacent layers, the energy for a single pancake vortex displaced by a distance r from the center of a magnetically coupled stack is[56]

$$U_c(r)=\frac{\Phi_0^2}{\pi\mu_0\Lambda}[\gamma+\ln(r/2\lambda_{ab})+K_0(r/\lambda_{ab})], \tag{16}$$

where $\Lambda=2\lambda_{ab}/d_s$ is the effective 2D screening length in a copper-oxide plane of thickness d_s, and γ is Euler's constant (≈ 0.5772). This activation energy reduces to

$$U_c(r)\approx\frac{\Phi_0^2}{4\pi\mu_0\Lambda}\left[\frac{r}{\lambda_{ab}}\right]^2 \tag{17}$$

in the limit of $r\ll\lambda_{ab}$. Because this energy is quadratic in the displacement, it predicts $U_{\rm pl}\propto 1/H$ rather than $U_{\rm pl}\propto 1/\sqrt{H}$. In addition, the magnitude of the kink energy is much less than that given by the anisotropic Ginzburg-Landau theory. Comparing Eqs. (11) and (17), we find

$$\frac{U_c(a_0)}{U_{\rm pl}}=\frac{a_0 d_s}{4\lambda_{ab}^2\ln(\tilde{\kappa})}\left[\frac{m_c}{m_{ab}}\right]^{1/2} \tag{18}$$

for $a_0<\lambda_{ab}$. Using typical values of $d_s=6$ Å, $\lambda_{ab}=2700$ Å, $\xi_{ab}=31$ Å, and $m_c/m_{ab}=6400$, the pancake double-kink energy is much less than the 3D double-kink energy for fields above $\approx 10^{-2}$ Oe. It is not surprising that the energy for shearing a stack of pancake vortices is less than that required for shearing a three-dimensional vortex because the pancake vortex model neglects the Josephson coupling energy. The energy required to displace a multiple-pancake section of a vortex should be even less than that required to displace a single pancake. This suggests that the 2D kink mechanism should dominate over 3D vortex kinks if the Josephson coupling energy between the Cu-O planes can be neglected.

The fact that the experimentally determined activation energies are much larger than that predicted by the two-dimensional model suggests that the Josephson coupling energy cannot be neglected in the field and temperature regime over which the activation energy was determined. This regime is plotted in Fig. 6 for sample MBE-1. In this figure, the low-temperature boundary (dashed line) is set by the lowest resistance that could be measured, and should not be interpreted as a change in physical behavior. However, the upper-temperature boundary marks the region over which Arrhenius plots of the resistive transitions became nonlinear. For fields below 2 T, the upper boundary corresponds to $\rho\geq 0.03\rho_n$. This is where conventional flux flow is thought to determine the resistance. However, for $H\geq 2$ T, the upper boundary corresponds to $\rho\geq 10^{-3}\rho_n-10^{-4}\rho_n$. These resistivities are too small to originate from conventional flux flow. However, it is possible that this high-field, high-temperature regime is where the 2D vortex motion dominates. Glazman and Koshelev[55] have predicted a cross over from 3D to 2D behavior in high fields even if the interlayer Josephson coupling is larger than the magnetic coupling. The crossover field is given by

$$B_{\rm cr}=\frac{2\pi\Phi_0}{d^2}\frac{m_{ab}}{m_c}\ln\left[\left[\frac{m_c}{m_{ab}}\right]^{1/2}\frac{d}{\xi_{ab}}\frac{1}{\sqrt{1+T/T_1}}\right], \tag{19}$$

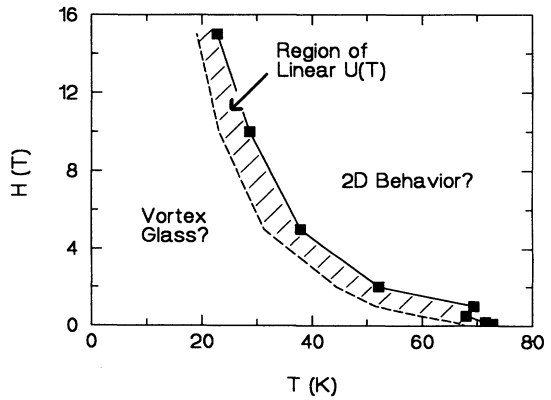

FIG. 6. Region of magnetic fields and temperatures over which the activation energy was determined for sample MBE-1.

where d is the interplanar spacing and $T_1 \approx 2\Phi_{05}^2 \xi_{ab}^2 / 16\pi^2 \lambda_c^2 d$. This gives crossover fields in the range of 1 to 3 T for $Bi_2Sr_2CaCu_2O_{8+\delta}$ at temperatures between 20 and 80 K. This is just the range of fields in which the high-resistance portions of the Arrhenius plots of the resistive transitions become nonlinear in all of the samples studied. It is possible that this regime is, therefore, dominated by thermal activation of 2D vortices. Using Clem's[56] calculations, the 2D vortices should give a $1/H$ field dependence to the activation energy in this regime. Of course, this neglects the Josephson coupling energy, and assumes that some other mechanism of flux motion does not have a lower energy than the double-kink activation previously described. Although the activation energies determined from the higher-resistance portions of the transitions are less than those determined from the lower-resistance portions of the transitions, it is difficult to determine the exact field dependence because of the nonlinearity of the Arrhenius plots in this regime.

If the above reasoning is correct, then the following picture emerges from the diagram in Fig. 6. At temperatures and magnetic fields above the shaded region, the vortices are two dimensional. As the temperature is lowered, there is a 2D to 3D transition at the solid line where the interlayer coupling begins to dominate. Within the shaded region the vortices are three dimensional, although we do not know how far down in temperature this regime extends because of the finite sensitivity of our measurements. Somewhere below the limits of our measurements is the proposed vortex-glass transition.[4,35,57] Although we have no direct evidence to support or refute the vortex-glass model, the observed 2D to 3D transition is a prerequisite for considering a 3D vortex glass in an intrinsically 2D material.

VI. CONCLUSIONS

We have measured the field-induced broadening of the resistive transitions of five $Bi_2Sr_2CaCu_2O_{8+\delta}$ thin films. Despite the wide variety of deposition techniques and surface morphologies, Arrhenius plots of the resistive transitions are qualitatively similar for all samples measured. This suggests the broadening is an inherent property of the material, and is not simply a result of sample inhomogeneities.

The lowest-resistance portions of the transitions are thermally activated with an activation energy well approximated by $U(H,T) \approx A(1-T/T_c)/\sqrt{H}$ over three decades of magnetic field. The activated model holds over approximately four orders of magnitude in resistance for $\mu_0 H \leq 1$ T, and for nearly two orders of magnitude in resistance for $\mu_0 H > 1$ T.

The activation energies for smooth, *in situ* films with critical currents above 10^6 A/cm^2 at 4.2 K are nearly twice as large as those for rough, *ex situ* films with critical currents of about 5×10^4 A/cm^2 at 4.2 K. This shows that increased surface roughness does not enhance flux pinning and suggests that U_0 correlates with J_c in our thin films. The activation energies in our films are much larger than those in bulk single crystals of the same material.

The field and temperature dependence of the activation energy, as well as its overall magnitude, is consistent with models by Geshkenbein *et al.*[37] and Vinokur *et al.*,[38] who claim that the activation energy arises from the thermally activated plastic shear deformations of a flux lattice, and a viscous flux liquid, respectively. Activation energies for smooth, high-J_c films (1740 K at 1 T) are within a factor of 2 of the value predicted by the models without any adjustable parameters.

The Geshkenbein and Vinokur models are shown to require less activation energy than direct lattice shear for our highly anisotropic $Bi_2Sr_2CaCu_2O_{8+\delta}$ films in the range of magnetic fields considered. This could explain why the activation energy in these films follows a different field dependence than the $1/H$ field dependence observed in $YBa_2Cu_3O_7$.

The magnitude and field dependence of the activation energy is much better predicted by 3D anisotropic Ginzburg-Landau theory than by 2D "pancake" vortices in the region of field and temperatures considered. The existence of 3D vortices in this regime is significant because it allows one to consider the possibility of a vortex glass in a system that was otherwise thought to be two dimensional.

ACKNOWLEDGMENTS

We would like to thank J. M. Graybeal for helpful discussions regarding the dimensionality of the vortices, and S. K. Anderson and I. D. Zitkovsky for technical assistance. This work was performed at the Center for Materials Science at MIT, which is supported by NSF/MRL No. DMR-87-19217, and at the Francis Bitter National Magnet Laboratory. Two of us (J.T.K. and T.P.O.) also acknowledge support from the Consortium for Superconducting Electronics through DARPA Contract No. MDA 972-90-C-0021.

*Present address: Department of Materials Science, Stanford University, Stanford, CA 94305.

†Department of Electrical Engineering and Computer Science, MIT, Cambridge, MA 02139.

[1]T. T. M. Palstra, B. Batlogg, R. B. van Dover, L. F. Schneemeyer, and J. V. Waszczak, Phys. Rev. B **41**, 6621 (1990).

[2]T. T. M. Palstra, B. Batlogg, L. F. Schneemeyer, and J. V. Waszczak, Phys. Rev. Lett. **61**, 1662 (1988).

[3]T. T. M. Palstra, B. Batlogg, R. B. van Dover, L. F. Schneemeyer, and J. V. Waszczak, Appl. Phys. Lett. **54**, 763 (1989).

[4]Daniel S. Fisher, Matthew P. A. Fisher, and David A. Huse, Phys. Rev. B **43**, 130 (1991).

[5]S. Martin, A. T. Fiory, R. M. Fleming, G. P. Espinosa, and A. S. Cooper, Appl. Phys. Lett. **54**, 72 (1988).

[6]For the purposes of this paper J_c will refer to the critical current density obtained from transport measurements using a 1 μV/cm voltage criterion.

[7]D. W. Face, J. T. Kucera, J. Crain, M. M. Matthiesen, D. Steel, G. Somer, J. Lewis, J. M. Graybeal, T. P. Orlando, and D. A. Rudman, IEEE Trans. Magn. **MAG-25**, 2341 (1989).

[8]D. W. Face, M. J. Neal, M. M. Matthiesen, J. T. Kucera, J. Crain, J. M. Graybeal, T. P. Orlando, and D. A. Rudman, Appl. Phys. Lett. **53**, 246 (1988).

[9]Figure 2b of Ref. 13 shows a scanning electron microscope (SEM) image of a typical *ex situ* film.

[10]D. W. Face, J. M. Graybeal, T. P. Orlando, and D. A. Rudman, Appl. Phys. Lett. **56**, 1493 (1990).

[11]I. D. Zitkovsky, Qing Hu, T. P. Orlando, J. Melngailis, and Tao Tao, Appl. Phys. Lett. **59**, 727 (1991).

[12]J. T. Kucera, D. G. Steel, D. W. Face, J. M. Graybeal, T. P. Orlando, and D. A. Rudman, Physica C **162-164**, 671 (1989).

[13]J. T. Kucera, L. M. Rubin, K. Uwai, J. D. Perkins, J. M. Graybeal, T. P. Orlando, J. B. Vander Sande, A. Roshko, and J. Moreland, Physica C **192**, 23 (1992).

[14]Figures 2a and 2c of Kucera *et al.* (Ref. 13) are SEM images of films similar to SPU-1 and SPU-2, respectively. These films do not show the voids, secondary phase particles, or grossly micaceous microstructure of films deposited at ambient temperature [Fig. 2b of Kucera *et al.* (Ref. 13)].

[15]J. N. Eckstein, I. Bozovic, D. G. Schlom, and J. S. Harris, Jr., Appl. Phys. Lett. **57**, 1049 (1990).

[16]J. N. Eckstein, I. Bozovic, K. E. von Dessonneck, D. G. Schlom, J. S. Harris, Jr., and S. M. Baumann, Appl. Phys. Lett. **57**, 931 (1990).

[17]J. N. Eckstein (unpublished).

[18]The surface morphology of MBE films is depicted in Fig. 2 of Eckstein *et al.* (Ref. 16).

[19]The zero-field critical current density was estimated from the J_c of 2×10^5 A/cm^2 at 4.2 K and $H=15$ T.

[20]H. H. Sample, B. L. Brandt, and L. G. Rubin, Rev. Sci. Instrum. **53**, 1129 (1982).

[21]The only exception was sample SPU-1, which was smooth and had a high J_c, but fell into the lower-energy class of films. This sample had a reduced transition temperature of 51 K. The lower activation energy observed in this film suggests that the activation energy scales with T_c.

[22]M. Tinkham, Phys. Rev. Lett. **61**, 1658 (1988).

[23]K. C. Woo, K. E. Gray, R. T. Kampwirth, J. H. Kang, S. J. Stein, R. East, and D. M. McKay, Phys. Rev. Lett. **63**, 1877 (1989).

[24]W. R. White, A. Kapitulnik, and M. R. Beasley, Phys. Rev. Lett. **66**, 2826 (1991).

[25]J. Z. Sun, K. Char, M. R. Hahn, T. H. Geballe, and A. Kapitulnik, Appl. Phys. Lett. **54**, 663 (1989).

[26]N. Kobayashi, H. Iwasaki, H. Kawabe, K. Watanabe, H. Yamane, H. Kurosawa, H. Masumoto, T. Hirai, and Y. Muto, Physica C **159**, 295 (1989).

[27]T. Fukami, T. Kamura, A. A. A. Youssef, Y. Horie, and S. Mase, Physica C **159**, 422 (1989).

[28]P. Mandal, A. Poddar, A. N. Das, and B. Ghosh, Physica C **169**, 43 (1990).

[29]D. Shi and M. S. Boley, Supercond. Sci. Technol. **3**, 289 (1990).

[30]A. A. A. Youssef, T. Fukami, and S. Mase, Solid State Commun. **74**, 257 (1990).

[31]B. Rakvin, T. A. Mahl, A. S. Bhalla, Z. Z. Sheng, and N. S. Dalal, Phys. Rev. B **41**, 769 (1990).

[32]S. Gygax, W. Xing, O. Rajora, and A. Curzon, Physica C **162-164**, 1551 (1989).

[33]E. J. Ansaldo, B. Batlogg, R. J. Cava, D. R. Harshman, L. W. Rupp, T. M. Riseman, and D. Williams, Physica C **162-164**, 259 (1989).

[34]M. V. Feigel'man and V. M. Vinokur, Phys. Rev. B **41**, 8986 (1990).

[35]H. Safar, P. L. Gammel, D. J. Bishop, D. B. Mitzi, and A. Kapitulnik, Phys. Rev. Lett. **68**, 2672 (1992).

[36]M. R. Beasley, R. Labusch, and W. W. Webb, Phys. Rev. **181**, 682 (1969).

[37]V. Geshkenbein, A. Larkin, M. Feigel'man, V. Vinokur, Physica C **162-164**, 239 (1989).

[38]V. M. Vinokur, M. V. Feigel'man, V. B. Geshkenbein, and A. I. Larkin, Phys. Rev. Lett. **65**, 259 (1990).

[39]R. E. Reed-Hill, *Physical Metallurgy Principles,* 2nd ed. (Van Nostrand, New York, 1973), p. 848ff.

[40]G. E. Dieter, *Mechanical Metallurgy,* 3rd ed. (McGraw-Hill, New York, 1986), p. 119.

[41]B. Batlogg, T. T. M. Palstra, L. F. Schneemeyer, R. B. van Dover, and R. J. Cava, Physica C **153-155**, 1062 (1988).

[42]D. E. Farrell, S. Bonham, J. Foster, Y. C. Chang, P. Z. Jiang, K. G. Vandervoort, D. J. Lam, and V. G. Kogan, Phys. Rev. Lett. **63**, 782 (1989).

[43]D. H. Kim, K. E. Gray, R. T. Kampwirth, and D. M. McKay, Phys. Rev. B **42**, 6249 (1990).

[44]D. E. Farrell, R. G. Beck, M. F. Booth, C. J. Allen, E. D. Bukowski, and D. M. Ginsberg, Phys. Rev. B **42**, 6758 (1990).

[45]S. Sriahar, D.-H. Wu, and W. Kennedy, Phys. Rev. Lett. **63**, 1873 (1989).

[46]Y. J. Uemura, L. P. Le, G. M. Luke, B. J. Sternlieb, W. D. Wu, J. H. Brewer, T. M. Riseman, C. L. Seaman, M. B. Maple, M. Ishikawa, D. G. Hinks, J. D. Jorgensen, G. Saito, and H. Yamochi, Phys. Rev. Lett. **66**, 2665 (1991).

[47]L. Krusin-Elbaum, R. L. Geeene, F. Holtzberg, A. P. Malozemoff, and Y. Yeshurun, Phys. Rev. Lett. **62**, 217 (1989).

[48]U. Welp, W. K. Kwok, G. W. Crabtree, K. G. Vandervoort, and J. Z. Liu, Phys. Rev. Lett. **62**, 1908 (1989).

[49]D. E. Farrell, C. M. Williams, S. A. Wolf, N. P. Bansal, and V. G. Kogan, Phys. Rev. Lett. **61**, 2805 (1988).

[50]J. D. Hettinger, A. G. Swanson, W. J. Skocpol, J. S. Brooks, J. M. Graybeal, P. M. Mankiewich, R. E. Howard, B. L. Straughn, and E. G. Burkhardt, Phys. Rev. Lett. **62**, 2044 (1989).

[51]O. Brunner, L. Antognazza, J.-M. Triscone, L. Miéville, and Ø. Fischer, Phys. Rev. Lett. **67**, 1354 (1991).

[52]A. R. Strnad, C. F. Hempstead, and Y. B. Kim, Phys. Rev. Lett. **13**, 794 (1964).

[53]Y. B. Kim, C. F. Hempstead, and A. R. Strnad, Phys. Rev. **139**, 1163 (1965).

[54]L. P. Gor'kov and N. B. Kopnin, Usp. Fiz. Nauk. **116**, 413 (1975) [Sov. Phys. Usp. **18**, 496 (1975)].

[55]L. I. Glazman and A. E. Koshelev, Phys. Rev. B **43**, 2835 (1991).

[56]J. R. Clem, Phys. Rev. B **43**, 7837 (1991).

[57]P. L. Gammel, L. F. Schneemeyer, J. V. Waszczak, and D. J. Bishop, Phys. Rev. Lett. **61**, 1666 (1988).